

Design and fabrication of step mirrors used in space-modulated Fourier transform infrared spectrometer

Ying Zheng,^{1,2} Jingqiu Liang,^{1,*} and Zhongzhu Liang^{1,3}

¹State Key Laboratory of Applied Optics, Changchun Institute of Optics, Fine Mechanics and Physics, Chinese Academy of Sciences, Changchun, Jilin, 130033, China

²Graduate School of Chinese Academy of Sciences, Beijing 100039, China

³liangzz@ciomp.ac.cn

*liangjq@ciomp.ac.cn

Abstract: A model of miniaturized space-modulated Fourier transform infrared spectrometer (FTIR) is given. The two step mirrors as the key components are designed and a lithography-electroplating technique used to fabricate the small step mirror is proposed. We analyze the effect of the experiment results resulted from fabricating technics on the recovery spectrum in theory, and demonstrate that the lithography-electroplating technique is an effective method to fabricate the step mirror, which make miniaturized FTIR realized. We believe that the performances of FTIR can be better realized by optimizing experimental conditions to make this fabricating method more attractive.

©2013 Optical Society of America

OCIS codes: (300.6190) Spectrometers; (300.6300) Spectroscopy, Fourier transforms; (230.4000) Microstructure fabrication.

References and links

1. K. D. Moeller, "Miniaturized wavefront-dividing interferometers without moving parts for field and space applications," *Proc. SPIE* **1992**, 130–139 (1993).
 2. K. D. Möller, "Wave-front-dividing array interferometers without moving parts for real-time spectroscopy from the IR to the UV," *Appl. Opt.* **34**(9), 1493–1501 (1995).
 3. F. Brachet, P. J. Hébert, E. Cansot, C. Buil, A. Lacan, L. Roucayrol, E. Courau, F. Bernard, C. Casteras, J. Loesel, and C. Pierangelo, "Static Fourier transform spectroscopy breadboards for atmospheric chemistry and climate," *Proc. SPIE* **7100**, 710019, 710019-11 (2008).
 4. A. Lacan, F. M. Bréon, A. Rosak, F. Brachet, L. Roucayrol, P. Etcheto, C. Casteras, and Y. Salaün, "A static Fourier transform spectrometer for atmospheric sounding: concept and experimental implementation," *Opt. Express* **18**(8), 8311–8331 (2010).
 5. E. V. Ivanov, "Static Fourier transform spectroscopy with enhanced resolving power," *J. Opt. A. Pure Appl. Opt.* **2**(6), 519–528 (2000).
 6. Y. M. Kong, J. Q. Liang, Z. Z. Liang, B. Wang, and J. Zhang, "Micro assembled Fourier transform spectrometer," *Proc. SPIE* **7283**, 728304, 728304-5 (2009).
 7. B. Wang, Z. Z. Liang, Y. M. Kong, J. Q. Liang, J. G. Fu, Y. Zheng, W. B. Zhu, J. G. Lv, W. B. Wang, P. Shu, and Z. Jun, "Design and fabrication of micro multi-mirrors based on silicon for micro-spectrometer," *Acta Phys. Sin.* **59**, 907–912 (2010).
 8. C. Feng, B. Wang, Z. Z. Liang, and J. Q. Liang, "Miniaturization of step mirrors in a static Fourier transform spectrometer theory and simulation," *J. Opt. Soc. Am. B* **28**(1), 128–133 (2011).
 9. C. Feng, J. Q. Liang, and Z. Z. Liang, "Spectrum constructing with nonuniform samples using least-squares approximation by cosine polynomials," *Appl. Opt.* **50**, 6377–6383 (2011).
 10. B. K. Avrit, E. W. Maxwell, L. M. Huynh, and E. S. Capsuto, "Characterization of an Ultra-Thick Positive Photoresist for Electroplating Applications," *Proc. SPIE* **5376**, 929–938 (2004).
-

1. Introduction

Recently, with the rapid growth of the demands in many areas such as chemical analysis, medicine testing, environmental monitoring and space detection, high-precision, light-weight and miniaturized Fourier transform spectrometer (FTS) are strongly needed, and the

development of micro-electrical mechanical systems (MEMS) technology makes it possible. Among various kinds of FTSs, space-modulated FTSs have many advantages over time-modulated FTSs due to its system stability and structure compaction. During past years, a space-modulated FTS based on classical Michelson interferometer with two plane mirrors replaced by two step mirrors was proposed by Moller [1,2], and later studied by some other institutions such as the Centre National d'Etudes Spatiales (CNES) in France [3,4] and EVI Research in Canada [5] including us [6–9]. This design allows for a relatively simple and portable instrument without moving parts.

According to Moller, the width of a facet should be more than 100 times the longest wavelength to be studied so that the diffraction effect would be negligible [1]. As the working wavelength ranges from mid-infrared to far-infrared, larger steps are needed. This brings potential drawbacks such as increasing volume and even mass. The edge-enlarge method proposed by Feng Cong *et al.* [8] overcame diffraction restriction to the size of step mirrors in middle and far-infrared. Hence, the step mirrors miniature is possible.

In this paper, the principle of a space-modulated Fourier transform infrared spectrometer (FTIR) based on step mirrors is reported, and the structure of the step mirrors is designed. In the works of Frank Brachet *et al.* [3,4], two step mirrors were made by molecular bounding technique, whereas it is helpless to the manufacture of smaller steps. A micromachining method is proposed to fabricate the small step mirror. This method makes full use of the MEMS advantages in precisely location. The photoresist patterning of AZ P4620 and the electroplating technology are used. The test results of step heights and surface roughness are given, and the effect on the recovery spectrum of manufacturing error and the reason for that are discussed. This paper is contributive to the realization of miniaturized FTIR and certainly valuable to the fabrication of mid-thick microstructures.

2. Principle of the FTIR

Figure 1 shows the simplified configuration of the micro FTIR. It consists of two mutually perpendicular step mirrors instead of two plane mirrors in conventional Michelson interferometer. As a matter of fact, two step mirrors form an optical path difference (OPD) array. Bisecting the small step mirror and the large step mirror is a beamsplitter, where a collimated beam of radiation from an external source can be partially reflected to the small step mirror and partially transmitted to the large step mirror. When the beams return to the beamsplitter, they interfere. Because of the effect of interference, the intensity of passing to the detector depends on the difference in path of the beams in the two arms of the interferometric system. The variation in the intensity of the beams passing to the detector as a function of the path difference ultimately yields the spectral information via Fourier transform.

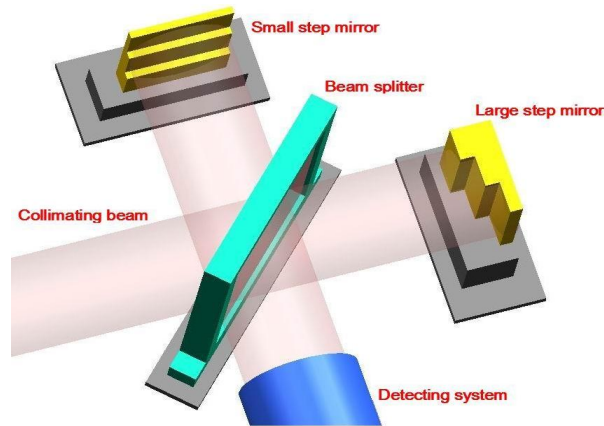


Fig. 1. Simplified configuration of the micro FTIR.

3. Design and fabrication of step mirrors

3.1. Design of step mirrors

Step mirrors play an important role in the realization of spectrometer performances. The structure of step mirror is shown in Fig. 2. H is the height of the step mirror, W is the width of the reflecting surface, and L_1 and L_2 is respectively the effective length and width of the step mirror. According to Nyquist sampling criterion, the sampling frequency must be greater than or equal to twice the Nyquist frequency, that is to say, the sampling interval is smaller than one second the minimum wavelength. In order to assure the OPD continuity, one step height of large step mirror is equal to the total height of the steps of small step mirror. For the range of the working wavelength from 3 to 5 μm , and the spectral resolving of excelled 8 cm^{-1} , the height of small step mirror H_1 is smaller than $0.75\text{ }\mu\text{m}$, and the sampling length should be larger than $1250\text{ }\mu\text{m}$. Considering the effect of diffraction and spectrum resolution, the width W of the reflecting surface in two step mirrors is both 1 mm , and the height H of two step mirrors are $0.625\text{ }\mu\text{m}$ and $20\text{ }\mu\text{m}$, respectively.

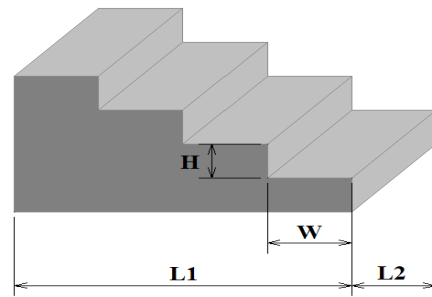


Fig. 2. Sketch map of step mirror.

3.2. Fabrication of step mirror

Considering the high dimension precision of step mirror, lithography-electroplating technique was developed to fabricate the small step mirror. At first, the substrate of step mirror was cleaned, and the mask pattern of the photoresist could be obtained on the special area of the substrate by lithography. Then, the process of electroplating and lift-off were used. After removing the photoresist, the two-step structure was obtained. We could get the structure of the small step mirror with 2^N steps by repeating N th these processes. After depositing or sputtering the infrared reflective film and protective film on the surface of small step mirror structure, the small step mirror was obtained.

The electroplating as a well-known technique in MEMS is proposed because of its simplicity, operating cost low, lower processing temperature, and controllable thickness. Several materials, such as nickel, copper, gold, or permalloy, are used to fabricate microstructures. Finally, Ni electroplating was chosen.

In the experiment, titanium (Ti) was used as the substrate with a length and width of 50 mm and a thickness of 2 mm. Because negative resists are very difficult to remove after electroplating due to their chemical composition, whereas positive resists do not have this issue [10], a UV positive type of photoresist AZ P4620 (AZ Electronic Materials, Japan) was chosen to fabricate the electroplating molds. After pretreatment of the substrate, spin coating was adopted with the spin machine KW-4A. Considering the requirement that the thickness of photoresist layer is greater than that of Ni film in the process of electroplating, we selected appropriate spin speed for different manufacturing step according to the curve of photoresist thickness vs spin speed shown in Fig. 3. Before exposure, the sample was prebaked on a hotplate with the temperature rising by way of “step by step” to remove the excessive solvent and improve the adhesion of the photoresist to the substrate as Fig. 4. At the same time, a proprietary edge bead reduction process resulting from this thick photoresist is necessary in order to get good contact during exposure. After exposure, the sample was subjected to develop in 0.5% NaOH at room temperature.

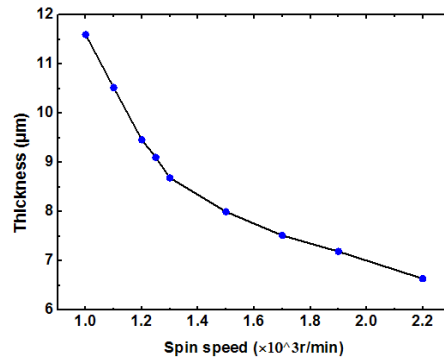


Fig. 3. The curve of spin speed vs. layer thickness.

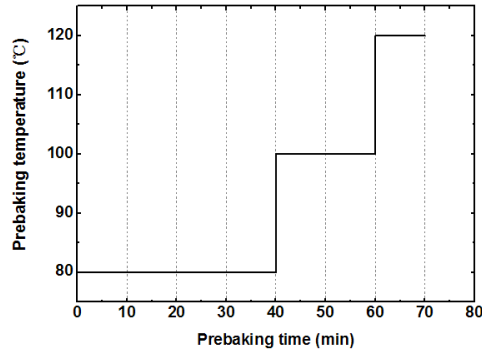


Fig. 4. The curve of prebaking time vs. temperature.

For the nickel electroplating process, a solution containing nickel sulfate ($\text{NiSO}_4 \cdot 6\text{H}_2\text{O}$, 250 g/L), nickel chloride (NiCl_2 , 30 g/L), boric acid (H_3BO_3 , 35g/L), and sodium lauryl sulphate ($\text{C}_{12}\text{H}_{25}\text{SO}_4\text{Na}$, 0.1 g/L) was used. A magnetic pellet was used to stir the solution to maintain the uniformity of the concentration. Because larger quantities of hydrogen evolution increase pH value of the solution adjacent to the cathode, the pH is usually adjusted to maintain the optimum value by the addition of dilute sulfuric acid (H_2SO_4). The effect created by other process parameters such as current density, electroplating time and temperature on

the surface quality of Ni film have also been investigated. Figures 5 and 6 presents the surface morphology at different current density and electroplating time respectively. It is obvious that the surface quality of Ni film declined when the current density or electroplating time increased at room temperature. The optimum parameters used for Ni electroplating are presented in Table 1. After electroplating, the remaining photoresist was removed by soaking the seed layer in an acetone bath until no trace of photoresist was observed, then the step structure appeared.

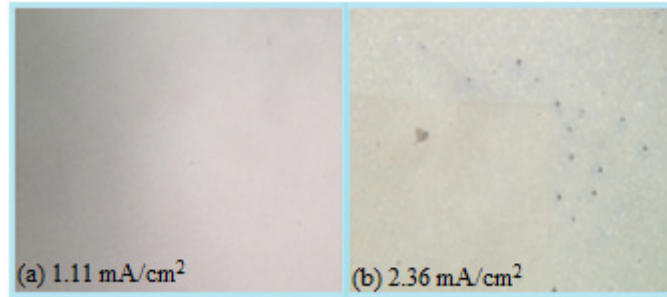


Fig. 5. Surface morphology at different current density (time = 3h, 400 ×).

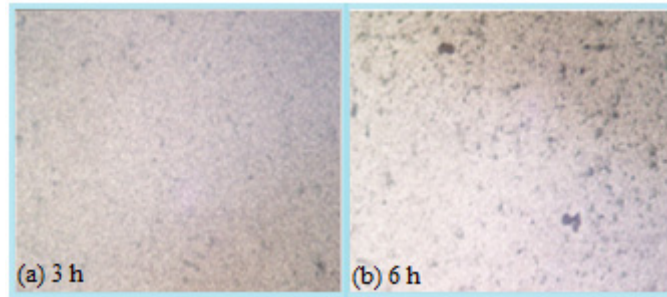


Fig. 6. Surface morphology at different electroplating time (current density = 1.28 mA/cm², 400 ×).

Table 1. Parameters of Ni Electroplating

Anode	Pure Nickel Plate (Ni:99.99%)
pH of Ni electrolyte	4.5-5.5
Temperature	Room Temperature
Current Density	1-2 mA/cm ²
Time of Ni electroplating	0.5-5 h

4. Results and discussion

Under aforementioned experimental conditions, the small step mirror with golden reflect coating was obtained as displayed in Fig. 7. Figures 8 and 9 presents one step profile and the root-mean-square (rms) values of the surface roughness measured by atomic force microscopy (AFM), respectively. Test results showed RMS of the reflect surface roughness in small step mirror is 67.408 nm. On the other hand, the RMS of reflect surface in large step mirror can be less than 5 nm according to our existing fabricated technology. Based on the above roughness values of two mirrors, a source of discrete wavenumbers (2000, 2500, 3300 cm⁻¹) (SD source) is simulated to test the effect of the roughness of reflective surface on the recovery spectrum as shown in Fig. 10. As can be observed from the figure, the real spectrum with the roughness of 67.408 nm and 5 nm (red line) nearly agrees with the ideal spectrum (blue line), that is to say, the reflected surface roughness of small step mirror manufactured by lithography-electroplating technique cannot affect the recovery spectrum.

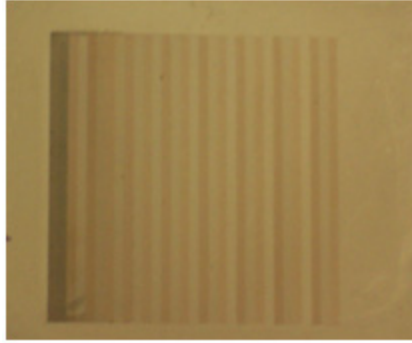


Fig. 7. Small step mirror with reflect coating.

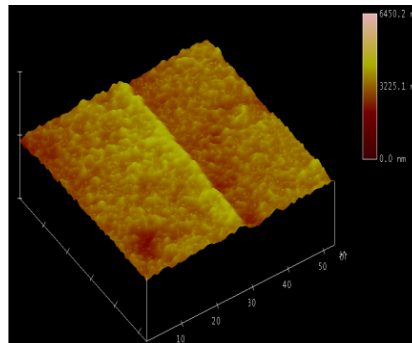


Fig. 8. One step of small step mirror by AFM.

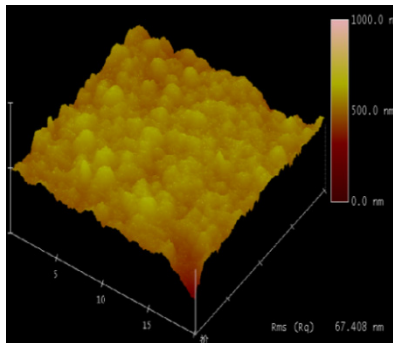


Fig. 9. AFM measurement of the reflect surface in small step mirror.

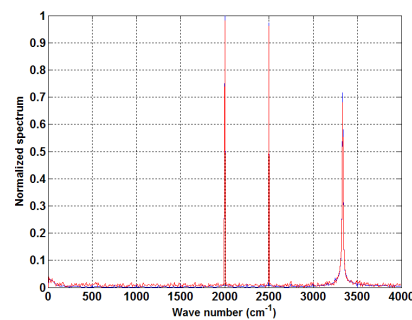


Fig. 10. Real spectrum with roughness 67.408 nm and 5 nm (red line) vs. ideal spectrum (blue line).

The step heights of the small step mirror were measured by KLA-Tencor P-16 + Surface profile as partly shown in Fig. 11. In the measurement, the length scanned by stylus tip covered with the transverse distance between the lowest step and the highest step, and scan speed and scan rate are 100 $\mu\text{m/s}$ and 200 HZ, respectively. As can be seen on this image, not all step surfaces is parallel to x -coordinate axis, which would make a result that the beams arrived at the step surfaces are not reflected perpendicularly, but with a minor angle. The primary reason for this case is that the substrate is not absolutely plane, in other words, it is difficult to achieve even surface in the substrate by electroplating, and the step height is much smaller compared with the substrate dimension of $50 \times 50 \text{ mm}^2$, the unevenness of the substrate surface is obviously shown on the step surfaces. We have simulated the same source of discrete wavenumbers (SD source) used above to analyze the effect of this minor angle on the recovery spectrum. Considering the tilt relativity between small step mirror and large step mirror, one of them analyzed is enough. Taking small step mirror with the rotation angle α as the example, it turns around on an axis which is vertical to the normal direction of reflect surface and the direction of long side L_2 . Figure 12 shows the ideal spectrum ($\alpha = 0$) versus the real spectrum ($\alpha = 0.01^\circ$). It can be seen from the Fig. 12 that the positions of wavenumber peaks shift to the long wavelength direction, and much noise is added on the spectrum. As a result, the signal to noise ratio decreased with increasing tilt angle α , as shown in Fig. 13. Although it is tolerable to the recovery of the spectrum within a certain range, reducing the tilt angle effects is necessary. Hence, further work needs to be done to optimized the conditions in order to get more parallel reflecting surface.

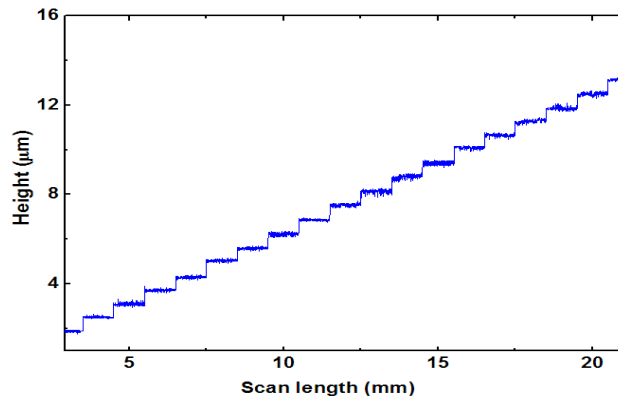


Fig. 11. Steps height of small step mirror tested by KLA-Tencor P-16 + profile.

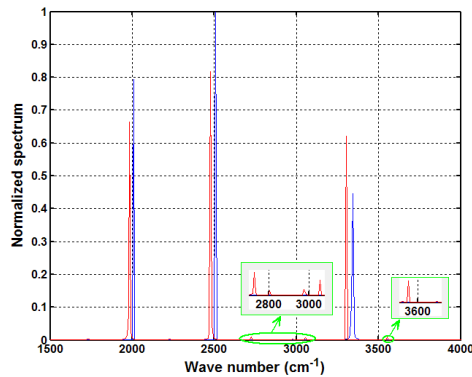


Fig. 12. Ideal spectrum ($\alpha = 0$) vs real spectrum ($\alpha = 0.01^\circ$).

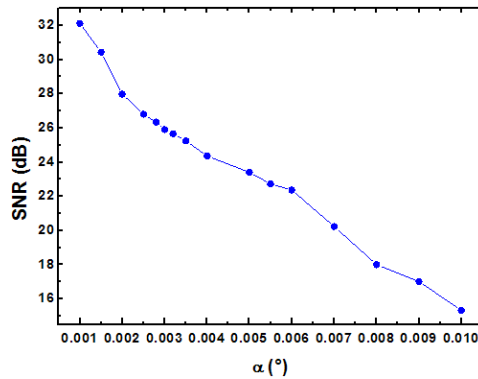


Fig. 13. SNR vs. α

Figure 14 shows the difference between each step height measured and ideal step height. The red solid circles are the measured step heights, and blue solid circles are the ideal step heights. Table 2 presents heights detail including maximal height (H_{Max}), minimal height (H_{Min}) and average height (H_{Ave}), along with the errors ($H_{MaxError}$, $H_{MinError}$ and $H_{AveError}$) compared with ideal step height. As can be seen from Table 2, the maximum error is less than 0.1 μm , and the average error of 0.2 nm is even smaller. The reason for the deviation between step height and ideal height can be explained from the fabricating technics. The conditions such as electroplating current density and temperature during the Ni electroplating could cause the asymmetric electric field distribution, which will surely bring the thickness ununiformity, especially from the second Ni film-deposited on, it is difficult to control the operating conditions to get the same layer thickness because part of the Ti substrate and part of Ni layer-deposited are put in the Ni electroplating solution. Hence, the manufacturing error of small step mirror must bring a nonuniform sampling problem, whereas the least-squares approximation of cosine polynomials (LSC) had proposed by our research team to construct the spectrum from the nonuniform samples of the interferogram, and proved the feasibility and the stability of the algorithm [9].

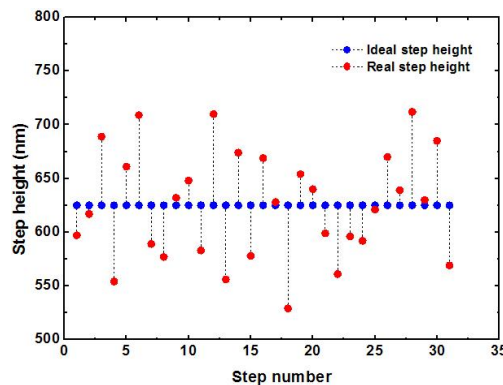


Fig. 14. Difference between real step height (red solid circle) and ideal step height (blue solid circle).

Table 2. Heights detail of small step mirror

Steps	$H_{Max}/H_{MaxError}$	$H_{Min}/H_{MinError}$	$H_{Ave}/H_{AveError}$
Value (nm)	712/+87	529/-96	624.8/0.2

5. Conclusion

In summary, it has been shown that a model of space-modulated Fourier transform infrared and the parameters of two step mirrors as the key parts in this interference system are given. Lithography-electroplating technique as an effective method for fabricating the small step mirror by the combination of standard lithography and electroplating was proposed and experimentally demonstrated. The contribution of the works lies in the fabrication of small step mirror by MEMS technology that makes miniaturized FTIR realized. This brings many advantages such as less volume and light weight.

Acknowledgments

The authors gratefully acknowledge the support of the National Natural Science Foundation of China (Grant No. 60977062, 61027010), the National High Technology Research and Development Program (863) of China (Grant No. 2009AA04Z315), the Scientific and Technological Development Project of Jilin Province, China (Grant No. 20120525), and the Scientific and Technological Development Project of Changchun city in Jilin province, China (Grant No. 11DJ03).